Simple correlated wave functions for the ground and some excited states of *sd* shell nuclei

J. Praena, E. Buendía, and F. J. Gálvez
Departamento de Física Moderna, Facultad de Ciencias, Universidad de Granada, E-18071 Granada, Spain

A. Sarsa
International School for Advanced Studies, SISSA, I-34014 Trieste, Italy

(Received 14 December 2002; published 2 April 2003)

Trial wave functions including angular momentum projection and deformation with central Jastrow and linear-type correlations are calculated to study the ground state rotational band of the ^{20}Ne, ^{24}Mg, ^{28}Si, ^{32}S, and ^{36}Ar nuclei and the ground state of ^{40}Ca. A systematic analysis of the competition among different correlation mechanisms on the binding energy and other properties such as the root mean square radius and the transition amplitudes of the rotational band is carried out. The one- and two-body radial densities and the momentum distribution are obtained. All the calculations have been performed by means of the variational Monte Carlo method.

DOI: 10.1103/PhysRevC.67.044301 PACS number(s): 21.60.−n, 21.10.−k, 27.30.+t, 02.70.Ss

I. INTRODUCTION

A thorough study of nuclear bound states starting from nucleon-nucleon interactions requires the inclusion of both short-range and medium- and large-range effects. Short-range correlations are due to the highly repulsive core of the nucleon-nucleon potential and are very important to reproduce correctly not only binding energies or internucleonic densities but also the tail of the momentum distribution, while at low momentum the mean field effects give the most important contribution [1]. The long-range effects are induced by collective excitations, pairing effects and/or mean field deformations. A microscopic description where both short- and long- and medium-range effects are included simultaneously is highly desirable. Typically and within the variational approach, these mechanisms are uncoupled in a factored trial wave function written as a correlation factor times a shell model term. The former is suited to take care of short-range correlations while the latter, usually named model wave function, is antisymmetric, provides the angular momentum of the state, and accounts for long-range effects. In some approximations the correlation factor is taken to be of Jastrow type [2,3] and the model function is a Slater determinant built from a given shell model.

One of the major drawbacks of this scheme is the computational difficulties involved in the calculation of the different expectation values. The technical problems have conveyed to the use of compact and simple wave functions. Often the simplifications have been focused on the model wave function. In many cases its role has been limited to be antisymmetric and to confine the nucleons. This gives rise to a poor description of medium- and long-range effects which are hard to account by means of the correlation factor. On the other hand, a wide variety of models including efficiently medium- and long-range effects have been devised as, for example, the SU3 Elliot model [4]. These models, however, have been mainly applied by using effective interactions with no core explicitly present.

Within the framework of the variational approach a factored trial wave function has been recently applied for *sp* shell nuclei [5,6]. One of the factors of such a trial wave function is built starting from the lowest order of the coupled cluster theory by imposing translational invariance and neglecting quadratic terms in the correlation function [7]. This leads to a linear factor times a model wave function written as a Slater determinant. This term can be understood as a compact way of doing a configuration interaction expansion of the model wave function. The model is completed by means of a Jastrow factor that includes higher order correlations. This scheme has been further generalized in order to better account for long-range effects by exploiting the freedom given by the model part of the trial wave function. For *sp* nuclei, model wave functions built using a deformed mean field with angular momentum projection [8] and including α-clustering effects [9,10] have shown to improve not only the binding energy but also other properties, giving rise to a qualitative better description of the nuclear bound states. Finally, it is worth mentioning here a recent work for *sp* shell nuclei where no Jastrow factor is used but the next order (quadratic) in the translationally invariant coupled cluster method has been implemented [11].

For medium and heavy nuclei, only Fermi hypernetted chain (FHNC) [12,13] and cluster expansion calculations with correlated wave functions have been carried out [14–16]. The aim of this work is to extend previous studies to *sd* shell spin and isospin saturated nuclei. This will provide a fully microscopic calculation for these nuclei by using a semirealistic nucleon-nucleon interaction of v_4 type. Accurate variational wave functions including a Jastrow term and a linear factor times a model wave function are obtained. The model wave function is built such that it provides the total angular momentum of the state under study and describes collective effects such as nuclear deformation. We shall focus on the interplay between the different correlation mechanisms induced in the trial wave function. Several nuclear properties such as the one- and two-body radial distributions and the single-particle momentum density are obtained, and the effects of the nucleon-nucleon correlations are discussed. The calculations are done for the ground state and its rotational band of the nuclei ^{20}Ne, ^{24}Mg, ^{28}Si, ^{32}S, and ^{36}Ar

TABLE I. Configuration and shape of the different nuclei studied. The orbitals are represented in the Cartesian basis (n_x, n_y, n_z). ^{16}O stands for the core $(000)^4(100)^4(010)^4(001)^4$.

Nucleus	Configuration	Shape
^{20}Ne	^{16}O, $(002)^4$	Prolate
^{24}Mg	^{16}O, $(101)^4(002)^4$	Triaxial
^{28}Si	^{16}O, $(110)^4(200)^4(020)^4$	Oblate
^{32}S	^{16}O, $(110)^4(101)^4(200)^4(020)^4$	Triaxial
^{36}Ar	^{16}O, $(110)^4(101)^4(011)^4(200)^4(020)^4$	Oblate
^{40}Ca	^{16}O, $(110)^4(101)^4(011)^4(200)^4(020)^4(002)^4$	Spherical

and also for the ground state of ^{40}Ca. All the calculations performed in this work are done by means of the variational Monte Carlo (VMC) method.

The structure of this work is as follows. In Sec. II, we show in detail the variational trial wave function used. Section III is devoted to the technical aspects involved in the calculation of the different properties. The results are presented and discussed in Sec. IV. Finally, the conclusions and perspectives of the present work can be found in Sec. V.

II. TRIAL WAVE FUNCTION AND NUCLEAR POTENTIAL

The trial wave function Ψ_{JKM} employed is factored into three terms and is built to have the total angular momentum of the state under study,

$$\Psi_{JKM}(1,\ldots,A) = F_{\mathcal{J}}(1,\ldots,A)F_{\mathcal{L}}(1,\ldots,A)\Phi_{JKM}(1,\ldots,A), \tag{1}$$

where J,K,M are angular momentum quantum numbers to be specified below. $F_{\mathcal{J}}$ and $F_{\mathcal{L}}$ stand for the Jastrow and the linear correlation factor, respectively, and $\Phi_{JKM}(1,\ldots,A)$ is the model wave function. The correlation factors are suited to deal with the short and medium correlation effects while the model wave function accounts for the antisymmetry and the angular momentum of the state.

The model wave function $\Phi_{JKM}(1,\ldots,A)$ is obtained through standard projection methods [17] as

$$\Phi_{JKM}(1,\ldots,A) = \frac{2J+1}{8\pi^2}\int d\Theta\, \mathcal{D}^{J*}_{MK}(\Theta)\mathbf{R}(\Theta)\Phi(1,\ldots,A), \tag{2}$$

where $\Phi(1,\ldots,A)$ is a Slater determinant that is the generator of the projected wave function and that we have called intrinsic wave function, and $\mathbf{R}(\Theta)$ is the rotation operator, $\mathcal{D}^{J*}_{MK}(\Theta)$ is the rotation matrix and Θ represents the Euler angles. The quantum number J gives the total angular momentum, K is its projection along the nuclear z axis, and M is the projection along the Z axis of the laboratory fixed frame. The resulting model wave function $\Phi_{JKM}(1,\ldots,A)$ is an eigenfunction of the total angular momentum operator. The correlation factors $F_{\mathcal{J}}$ and $F_{\mathcal{L}}$ are taken to be rotationally invariant and therefore commute with the projection operators. The possible values for K and J depend on the transformation properties under rotations of the intrinsic wave function Φ.

To construct the Slater determinant Φ in Eq. (2), we use the orbitals obtained from a Cartesian harmonic oscillator potential. The three Cartesian oscillator coefficients $(\alpha_x,\alpha_y,\alpha_z)$ are treated as variational parameters. Each spatial orbital is filled with four nucleons because we are dealing with the ground state and its rotational band for $A=4n$, $N=Z$ nuclei. All of these states have total spin $S=0$ and total isospin $T=0$. In Table I we show the configuration and symmetry considered for the nuclei studied in this work. They provide the lowest energy in a deformed Hartree-Fock framework with effective nucleon-nucleon interactions [18] and in a microscopic calculation using the Brink-Boecker interaction [16]. The configurations in Table I have in general nonspherical intrinsic shapes, even if the harmonic oscillator wave functions have spherical symmetry. For a more complete and coherent description we consider the three possible cases: (a) for spherical shape, a harmonic oscillator with $\alpha\equiv\alpha_x=\alpha_y=\alpha_z$, (b) for axial symmetry, a deformed harmonic oscillator with $\alpha\equiv\alpha_x=\alpha_y\neq\alpha_z$ with either prolate, $\alpha_z<\alpha$, or oblate, $\alpha_z>\alpha$, shape and (c) for triaxial shape, a deformed harmonic oscillator with all the three parameters different. For the axially symmetric nuclei we use the deformation parameter $d=\alpha_z/\alpha$ whereas for triaxial nuclei we use $d_y=\alpha_y/\alpha_x$ and $d_z=\alpha_z/\alpha_x$.

The Φ proposed in Table I for the different nuclei is not an eigenstate of the total angular momentum operator except for the spherical nucleus ^{40}Ca. The ground state wave function is obtained for all nuclei by using Eq. (2) with $K=0$ and $J=0$. In addition, for nonspherical configurations, the Φ function has no-null projection for $K=0$ and $J=2,4,6,\ldots$ that we have used here to describe the ground state rotational band of the corresponding nuclei. All the states here considered have even parity because Φ is an even function.

The Jastrow factor $F_{\mathcal{J}}$ is suited to account for the short-range correlations, whereas the linear factor $F_{\mathcal{L}}$ is obtained from the lowest order of the coupled cluster theory when both rotational and translational invariances are imposed [7]. Then, the linear factor can be thought as a compact way of carrying out a configuration interaction expansion of the trial wave function or as a linearization of the Jastrow term. These two correlation factors are taken here as

$$F_{\mathcal{J}}(1,\ldots,A)=\prod_{i<j}^{A} f(r_{ij}), \qquad F_{\mathcal{L}}(1,\ldots,A)=\sum_{i<j}^{A} g(r_{ij}). \tag{3}$$

Both correlation functions $f(r)$ and $g(r)$ are obtained by minimizing the expectation value of the nuclear Hamiltonian. To accomplish this, the following parametrization has been employed:

$$f(r)=1+\sum_{n=1}^{N} a_n e^{-b_n r^2}, \quad g(r)=\binom{A}{2}^{-1}+\sum_{m=1}^{M} c_m e^{-d_m r^2}, \tag{4}$$

where a_n, b_n, and d_m are nonlinear variational parameters fixed by using a simplex algorithm [19]. The variational energy is a quadratic form in c_m and therefore these parameters are calculated by solving a generalized eigenvalue problem. In this work, we have found that convergence within the statistical error is achieved with $N=2$ and $M=2$. In addition a good approximation is to take $d_m=b_m$, which will be the approximation used except in the model $\mathcal{L}_o$ described below. Another possibility that will be studied is to consider $F_{\mathcal{L}}$ as a direct linearization of the Jastrow factor.

For the nuclear interaction we use the modified Afnan-Tang potential MS3. This is a semirealistic interaction with an important repulsive core which has been developed to reproduce the *s*-wave scattering data up to about 60 MeV for the α particle [20]. It was originally defined only in the even channels and it was modified later on [21] by adding a repulsive part in the singlet- and triplet- odd components. This is a v_4-type potential containing spin exchange, isospin exchange, and spin-isospin exchange channels. It is a relatively simple potential that allows for accurate calculations [5,6] and provides a reasonable description of light and medium nuclei. These interactions are also useful to carry out a systematic analysis of the effects of the different correlation mechanisms included in the different properties calculated. An insightful analysis of the importance of the nuclear force models in the spectra of light nuclei, up to ten nucleons, from simple interactions that are purely central scalar to realistic models with 18 channels and accurate three-body potentials can be found in Ref. [22].

III. VMC CALCULATION OF THE MATRIX ELEMENTS

The optimization of the energy and the calculation of the different nuclear properties studied in this work has been carried out by means of the variational Monte Carlo method. The integral involved in the angular momentum projection, Eq. (2), is partially done by using the VMC algorithm. This gives rise to some differences with respect to standard implementations [23].

The expectation value of the Hamiltonian **H** can be written after some analytic manipulations as

$$E=\frac{\int d\Theta \quad \mathcal{D}^{(J)*}_{0,0}(\Theta)\langle\Phi|F_{\mathcal{J}}F_{\mathcal{L}}\mathbf{H}F_{\mathcal{L}}F_{\mathcal{J}}\mathbf{R}(\Theta)|\Phi\rangle}{\int d\Theta \quad \mathcal{D}^{(J)*}_{0,0}(\Theta)\langle\Phi|F_{\mathcal{J}}F_{\mathcal{L}}F_{\mathcal{L}}F_{\mathcal{J}}\mathbf{R}(\Theta)|\Phi\rangle}. \quad (5)$$

This expression can be obtained [8] by using the general properties of the rotation matrices and operators and by taking into account that both the Hamiltonian and the norm are zero rank tensors. If the Φ function has an axial symmetry the integration over the α and γ Euler angles is performed analytically, and there only remains the integration over the β angle around the *y* axis to be done with the VMC method.

The integrals in Eq. (5) not evaluated analytically will be calculated by using the VMC method. In doing so, it is convenient to use the following notation:

$$\frac{\langle f\rangle_\omega}{\langle g\rangle_\omega}=\frac{\int d\tau f(\tau)\omega(\tau)}{\int d\tau g(\tau)\omega(\tau)}, \quad (6)$$

where τ stands for both the spatial and intrinsic degrees of freedom of the nucleons and the Euler angles, and $\omega(\tau)$ is the so called probability density distribution which is required to be positive in the integration domain. The different terms in the integrals of Eq. (5) are not positive in the domain, and therefore a selection for $\omega(\tau)$ must be done. We have verified that a suitable choice is

$$\omega(1,\ldots,A;\Theta)=|\Phi F_{\mathcal{J}}F_{\mathcal{L}}\ F_{\mathcal{L}}F_{\mathcal{J}}\mathbf{R}(\Theta)\Phi|. \quad (7)$$

This scheme is also valid to calculate the expectation value of operators that do not transform as scalar under rotations. The algorithm, however, requires some modifications when expectation values between different wave functions are computed. This is the case of the reduced transition probability between the excited state 2^+ and the ground state given by

$$B(2^+\rightarrow 0^+;2)=\frac{1}{2J_i+1}|\langle\Psi_0||\mathbf{Q}_{20}||\Psi_2\rangle|^2, \quad (8)$$

where $\mathbf{Q}_{20}$ is the quadrupole operator. In this case the probability distribution function includes the wave functions of the two states involved in the calculation.

Further quantities that are evaluated in this work are the ground state spherically averaged one- and two-body radial distribution functions defined as

$$\rho_1(r)=\frac{1}{A}\frac{\langle\Psi|\sum_{i=1}^{A}\frac{1}{r^2}\delta(r-|\vec{r}_i-\vec{R}|)|\Psi\rangle}{\langle\Psi|\Psi\rangle}, \quad (9)$$

$$\rho_2(r_{12})=\frac{2}{A(A-1)}\frac{\langle\Psi|\sum_{i<j}^{A}\frac{1}{r_{12}^2}\delta(r_{12}-|\vec{r}_{ij}|)|\Psi\rangle}{\langle\Psi|\Psi\rangle}, \quad (10)$$

where $\vec{R}=1/A\Sigma_{i=1}^{A}\vec{r}_i$ is the center of mass coordinate. These functions provide the probability density distribution for finding a nucleon around the center of mass of the system or around another given nucleon, respectively. These densities are calculated here by using the algorithm previously described.

The momentum distribution function is defined as the Fourier transform of the one-body density matrix

$$n(\vec{k})=\int d\vec{r}_1 d\vec{r}_1'\rho(\vec{r}_1,\vec{r}_1')e^{i\vec{k}\cdot(\vec{r}_1-\vec{r}_1')}. \quad (11)$$

To calculate the spherically averaged momentum density we have worked as in Ref. [6]. For large-*k* values, the numerical estimation of the momentum distribution is affected by oscillations because of the $\sin(k|\vec{r}-\vec{r}'|)$ term in the integral. In order to get a reliable description in that region we have

TABLE II. Ground state energy (in MeV) and root mean square radius (in femtometer) for the ^{20}Ne nucleus. The calculation has been done for the MS3 potential. The Jastrow parameters $(a_1,b_1)=(0.56,0.75)$ and $(a_2,b_2)=(-1.20,1.53)$ are the same in the $\mathcal{J}$ and $\mathcal{JL}_o$ models. The oscillator parameter α is in fm^{-1}, and the parameters b_k and d_k in fm^{-2}. σ stands for the statistical error on each quantity.

	$E\pm\sigma$	$\sqrt{\langle r^2\rangle}\pm\sigma$	α	d_z
$\mathcal{J}$	-126.42 ± 0.17	2.65 ± 0.07	0.65	0.79
$\mathcal{L}_j$	-83.08 ± 0.15	2.68 ± 0.07	0.65	0.79
$\mathcal{L}_o$	-100.34 ± 0.27	2.79 ± 0.07	0.61	0.81
$\mathcal{JL}_o$	-127.33 ± 0.11	2.66 ± 0.07	0.65	0.79
	(c_1,d_1)	(c_2,d_2)		
$\mathcal{L}_j$	(0.56,0.75)	$(-1.20,1.53)$		
$\mathcal{L}_o$	(0.67,0.82)	$(-1.56,1.66)$		
$\mathcal{JL}_o$	$(-0.0068,0.75)$	$(-0.056,1.53)$		

fitted the VMC calculated momentum distribution to a linear combination of products of Gaussian functions by powers in *k*. This functional form for the momentum distribution arises when noncorrelated wave functions are used and also in correlated schemes with a Jastrow factor in both, when using a natural orbital representation at the lowest orders for the correlated wave function [24] and at the second order of the cluster expansion [25]. This scheme has shown to work properly for nuclei up to ^{16}O [6] and for the electronic distribution of atoms [26] but with a different parametrization because of the different form of the interaction.

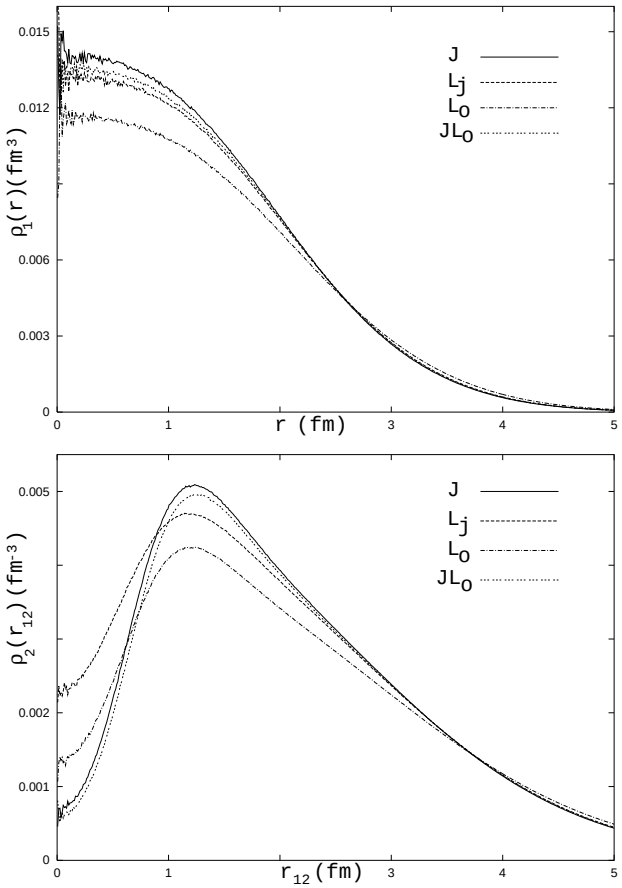

FIG. 1. Spherically averaged one- and two-body densities for ^{20}Ne calculated from different approximations.

IV. RESULTS

The linear correlation factor $F_{\mathcal{L}}$ in Eq. (3) can be understood as a linear approximation to the Jastrow factor. In order to elucidate the relation between these two correlation terms we have carried out a set of calculations with different trial wave functions that are particular cases of Eq. (1). First, an optimization of a variational wave function including only a Jastrow factor has been performed and the results are denoted as $\mathcal{J}$. Second, two different calculations with only the linear correlation factor have been carried out. The first one, labeled $\mathcal{L}_j$, is done by a straightforward linearization of the Jastrow factor obtained previously. In the second case, denoted $\mathcal{L}_o$, all the free parameters of the linear factor are fully optimized along with the model wave function. This will inform us about the validity of considering the linear factor simply as a linear approximation to the Jastrow term. Finally, these results are compared with the full trial wave function containing both the linear and the Jastrow terms, $\mathcal{JL}_o$. The ground state energy, the root mean square radius, and the parameters of the different trial wave functions are reported in Table II. Note that the Jastrow factor used in the $\mathcal{JL}_o$ model is the same as in the $\mathcal{J}$ model and that the nonlinear parameters of $F_{\mathcal{L}}$ in the $\mathcal{JL}_o$ model are taken as $d_m=b_m$, $m=1,2$. Therefore only the linear parameters in the linear correlation function are again optimized. This does not correspond to a complete optimization of the wave function, but we have verified that the results so obtained are very similar to those provided by a full optimization. The results are shown only for ^{20}Ne because the conclusions that can be drawn for this case are similar to those for the other nuclei.

The wave function $\mathcal{L}_j$ provides 65% of the binding energy while $\mathcal{L}_o$ provides 80%. This may indicate that there are some important effects in the linear correlation term not accounted by a straightforward linearization of the Jastrow factor. A more detailed analysis of the results shows that this difference is mainly due to the enhancement of the nuclear size in the $\mathcal{L}_o$ approximation that favors the core of the interaction to be avoided. A comparison of the $\mathcal{J}$ and $\mathcal{JL}_o$ binding energies shows that the mechanisms included by the linear term and not by the Jastrow factor have very little influence, lower than 1% in this case.

The study of the one- and two-body radial densities give us further insight on the different correlation mechanisms included by the variational wave functions. The one- and two-body densities for ^{20}Ne calculated from the different approximations analyzed here are plotted in the upper and lower panels of Fig. 1, respectively.

The one-body density is similar for the different approximations with the exception of the $\mathcal{L}_o$ model. This is because the parameters which characterize both the shell model and the correlation factor are very different in this model as compared to the others (see Table II), leading to a redistribution

TABLE III. Ground state energy (in MeV) and root mean square radius (in femtometer). The oscillator parameter α_x is in fm^{-1}. σ stands for the statistical error on each quantity.

Nucleus	Approx.	α_x	d_y	d_z	$E \pm \sigma$	$\sqrt{\langle r^2 \rangle} \pm \sigma$
^{24}Mg	$\mathcal{J}_{\mathrm{Ne}}$	0.59	1.12	0.86	-155.12 ± 0.25	2.80 ± 0.09
	$\mathcal{JL}_{\mathrm{Ne}}$	0.59	1.12	0.86	-156.31 ± 0.23	2.81 ± 0.09
	$\mathcal{J}$	0.58	1.17	0.84	-155.49 ± 0.21	2.84 ± 0.09
	$\mathcal{JL}_o$	0.58	1.17	0.84	-156.51 ± 0.19	2.85 ± 0.09
^{28}Si	$\mathcal{J}_{\mathrm{Ne}}$	0.52	1.0	1.30	-192.40 ± 0.17	2.94 ± 0.05
	$\mathcal{JL}_{\mathrm{Ne}}$	0.52	1.0	1.30	-193.89 ± 0.14	2.95 ± 0.05
	$\mathcal{J}$	0.54	1.0	1.30	-194.54 ± 0.17	2.89 ± 0.05
	$\mathcal{JL}_o$	0.54	1.0	1.30	-195.25 ± 0.19	2.87 ± 0.05
^{32}S	$\mathcal{J}_{\mathrm{Ne}}$	0.52	1.10	1.23	-229.28 ± 0.33	2.88 ± 0.09
	$\mathcal{JL}_{\mathrm{Ne}}$	0.52	1.10	1.23	-232.35 ± 0.35	2.93 ± 0.10
	$\mathcal{J}$	0.53	1.10	1.33	-232.42 ± 0.28	2.92 ± 0.08
	$\mathcal{JL}_o$	0.53	1.10	1.33	-233.11 ± 0.27	2.90 ± 0.09
^{36}Ar	$\mathcal{J}_{\mathrm{Ne}}$	0.56	1.0	1.11	-280.29 ± 0.30	2.88 ± 0.10
	$\mathcal{JL}_{\mathrm{Ne}}$	0.56	1.0	1.11	-284.54 ± 0.36	2.92 ± 0.11
	$\mathcal{J}$	0.58	1.0	1.15	-284.92 ± 0.26	2.83 ± 0.08
	$\mathcal{JL}_o$	0.58	1.0	1.15	-285.95 ± 0.34	2.84 ± 0.08
^{40}Ca	$\mathcal{J}_{\mathrm{Ne}}$	0.57	1.0	1.0	-336.21 ± 0.19	2.93 ± 0.03
	$\mathcal{JL}_{\mathrm{Ne}}$	0.57	1.0	1.0	-341.63 ± 0.17	2.97 ± 0.03
	$\mathcal{J}$	0.61	1.0	1.0	-345.34 ± 0.19	2.87 ± 0.03
	$\mathcal{JL}_o$	0.61	1.0	1.0	-346.53 ± 0.20	2.85 ± 0.03

of the nucleons to avoid the core of the potential, which is not killed by a Jastrow factor.

The two-body density shows a minimum located at the origin and a maximum around $r_{12}=1$ fm, i.e., where the nuclear potential is stronger. The two models including the Jastrow factor provide a very similar two-body density, which is very different from that obtained in any of the other two linear models. In those linear models the minimum at the origin is noticeably greater than in the other two cases because the linear correlation factor is not as efficient as the Jastrow term to deal with the core of the nuclear interaction. The $\mathcal{L}_o$ model, where the best linear factor is employed, gives a two-body density that is closer to that provided by the wave functions including the Jastrow term, showing a substantial reduction of the value at the origin as compared with the result from $\mathcal{L}_j$. Another interesting feature is that for large nucleon-nucleon distances the pair distribution function calculated from the $\mathcal{L}_o$ model is the biggest one. Finally, the effect of the linear term when the Jastrow factor is present is given by comparing the results provided by $\mathcal{JL}_o$ and $\mathcal{J}$. The pair distribution is reduced for short nucleon-nucleon separations when the linear term is present while the opposite holds at large distances.

In Table III, we report the results obtained for both the ground state energy and the root mean square radius of the rest of the nuclei studied here. We have not included the values without the Jastrow term because, as we have seen for ^{20}Ne, the binding energy is very small. In this table two sets of results are reported. The first one consists of $\mathcal{J}_{\mathrm{Ne}}$ and $\mathcal{JL}_{\mathrm{Ne}}$, and corresponds to a calculation in which the Jastrow correlation factor obtained for ^{20}Ne has been used for the rest of the nuclei. In the $\mathcal{JL}_{\mathrm{Ne}}$ model the linear coefficients of the linear correlation factor are the only ones optimized. The second set comprises $\mathcal{J}$ and $\mathcal{JL}_o$. The Jastrow correlation factor has been optimized for each nucleus. Then it has been used in the $\mathcal{JL}_o$ model in which the linear coefficients of the linear correlation factor are again optimized. It is worth noting that the correlation factor of ^{20}Ne provides accurate results for the other nuclei, but, as it could be expected, the quality of the results obtained by using this correlation factor decreases with the increase of number of nucleons, being the greater relative difference of 1.5% for ^{36}Ar and 3% for ^{40}Ca if the $\mathcal{J}_{\mathrm{Ne}}$ model is considered. However, the results from the model $\mathcal{JL}_{\mathrm{Ne}}$ approach much more to the full optimized results, except for ^{40}Ca for which a difference of ≈ 5 MeV still remains. For this nucleus there exists a FHNC calculation [12] obtained by using the same potential employed here. The result for the energy reported in that work, $E=-340.1$ MeV, is consistent with ours. Therefore, the linear correlation factor can adapt itself to the Jastrow factor of the ^{20}Ne nucleus to provide results for the energy of similar quality as in the $\mathcal{JL}_o$ model. However, there appears some appreciable differences in the root mean

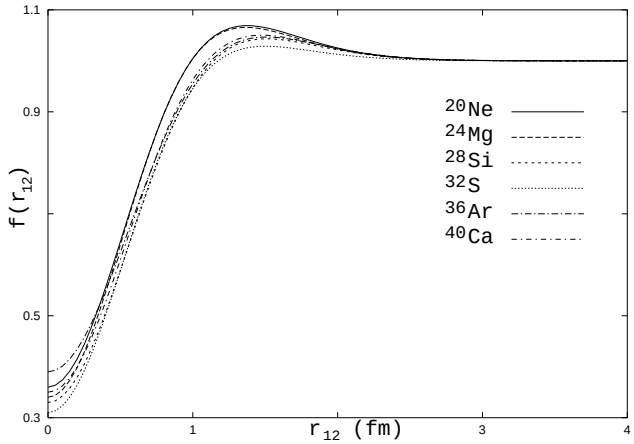

FIG. 2. Optimal Jastrow function for the different nuclei studied in this work.

square radius. To better illustrate the dependence of the correlation factor on the number of nucleons, we compare in Fig. 2 the Jastrow function for the different nuclei studied. As can be seen the dependence of this function on A is very small.

In the upper panel of Fig. 3 we plot the one-body density for all the nuclei considered. We show the results obtained starting from the best variational wave function obtained in this work, i.e., $\mathcal{JL}_o$. In the lower panel we plot the radial difference function

$$\Delta\rho_1(r) = r^2[\rho_1^{JL_o}(r) - \rho_1^{nc}(r)], \tag{12}$$

where $\rho_1^{JL_o}(r)$ and $\rho_1^{nc}(r)$ stand for the one-body density calculated from $\mathcal{JL}_o$ and from the uncorrelated trial wave function, respectively. This uncorrelated wave function is simply the model wave function of the $\mathcal{JL}_o$ parametrization.

As it is known, the correlation effects are very small for the one-body density. For the lighter nuclei the correlated single-particle density is higher than the uncorrelated one for low values of r and smaller for higher values of r. As the number of nucleons increases, the contrary tends to hold. Therefore, the single-particle density is mainly fixed by the model wave function, giving rise to quite different values for the different nuclear species. These results support the use of harmonic oscillator parameters fixed by fitting the root mean square radius or another single-particle quantity to the either experimental values or to the results from accurate realistic calculations.

In Fig. 4 we plot the two-body density for all of the nuclei studied calculated from the $\mathcal{JL}_o$ trial wave function. In the lower plot we show the difference between this density and the uncorrelated one, i.e., $\Delta\rho_2/r_{12}^2$.

The qualitative behavior of both the two-body density and the difference function is the same for all of the nuclei considered. The two-body density has a minimum at $r_{12}=0$, with a value that is nearly independent of the number of nucleons. The maximum is located in the region where the potential is stronger. The strength of such a maximum decreases as the number of nucleons increases. With respect to

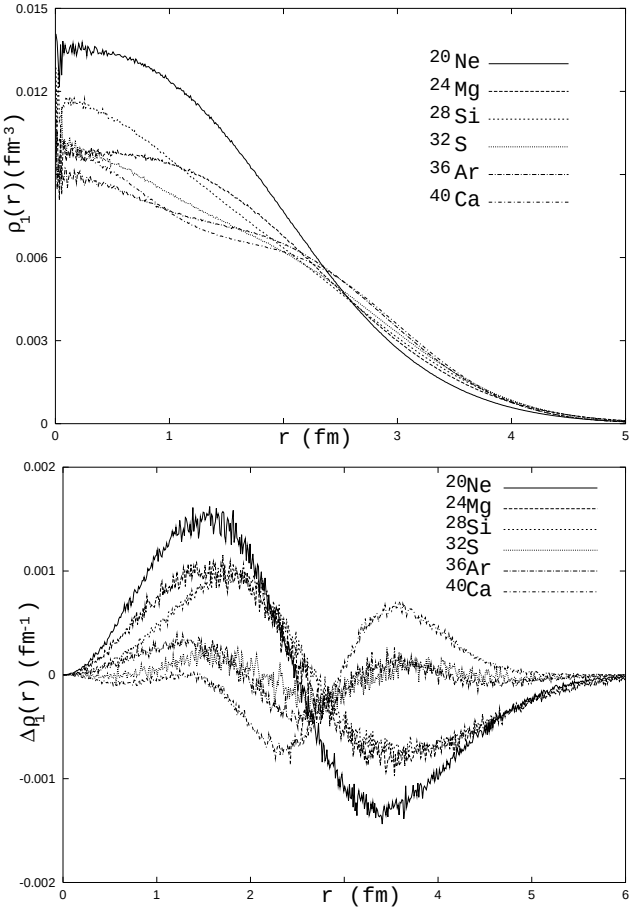

FIG. 3. Upper panel: One-body density for all the nuclei studied calculated from the best wave function obtained in this work, $\mathcal{JL}_o$. Lower panel: radial difference function $\Delta\rho_1(r)$.

the difference function, the main effects of correlations are at short distances as should be expected. There is also an appreciable mass distribution at medium and long separations that is different for each nucleus.

We have also calculated the spherically averaged momentum distribution $n(k)$, and analyzed the effects that correlations have on it. In Fig. 5 we plot the momentum distribution at low k for the nuclei here studied obtained from the $\mathcal{JL}_o$ trial wave function.

In this region, the momentum distribution is governed by the model part of the wave function giving rise to important differences between the different nuclei. For the configurations here used the greater the momentum density at the origin, the smaller the number of nucleons, except for ^{24}Mg.

As it is known [1], the most important effects of the nucleon-nucleon short-range correlations on the momentum distribution take place for large-k values. In Fig. 6 we plot in a semilogarithmic scale the momentum distribution for the different nuclei here studied calculated from the $\mathcal{JL}_o$ trial wave function. For ^{40}Ca we also plot the experimental results taken from Ref. [24]. For the nuclei ^{24}Mg to ^{40}Ca we also show the theoretical results of Moustakidis and Massen [25] calculated analytically at the second order of the cluster expansion from a wave function including a Jastrow factor and a model function part. In that calculation both terms

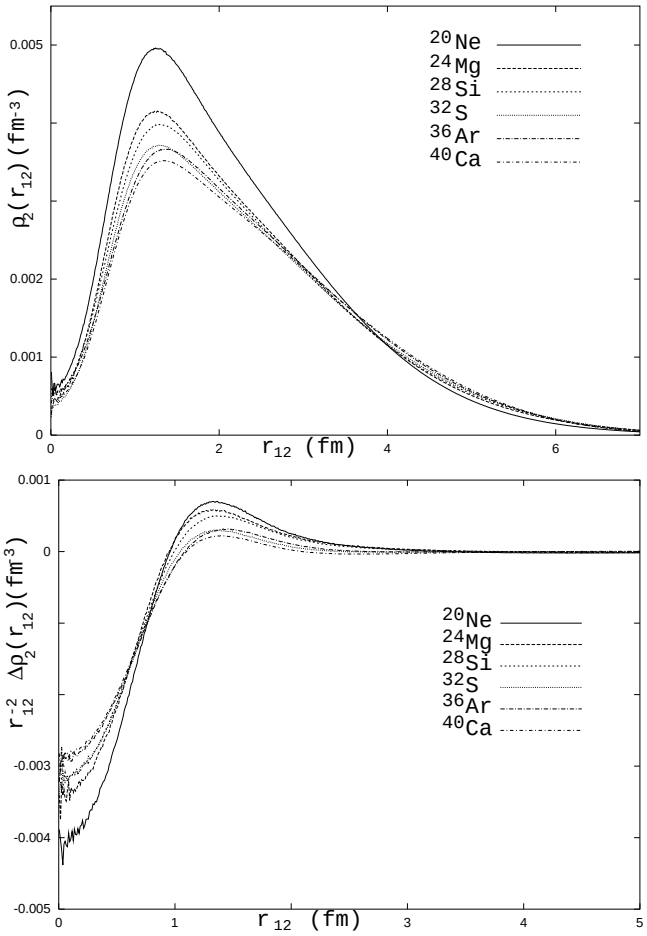

FIG. 4. Upper panel: Two-body density for all the nuclei studied calculated from the best wave function obtained in this work, $\mathcal{JL}_o$. Lower panel: difference function $\Delta\rho_2/r_{12}^2$ for all the nuclei considered.

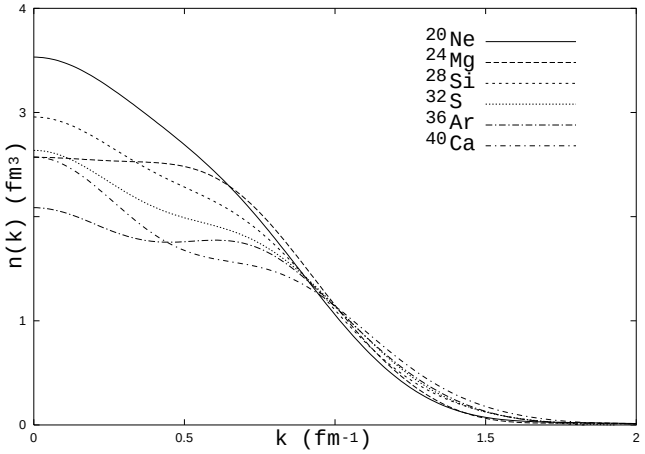

FIG. 5. Momentum distribution for all the nuclei studied calculated from the best wave function obtained in this work, $\mathcal{JL}_o$.

were parametrized and the values were fixed by fitting the experimental charge form factor.

The results of Ref. [25] present a good agreement with the fully microscopic results of this work. For $k \gtrsim 2$ fm^{-1} the effects of the correlations are more important, in such a way that the uncorrelated density is several order of magnitude lower than the corresponding correlated value. The correlations are also responsible for the change in the slope at $k \sim 2$ fm^{-1}. It is also worth mentioning the good agreement with the experimental results for ^{40}Ca in spite of the fact that the nucleon-nucleon force employed in this work cannot be considered as realistic.

State dependent correlations are not included in the variational trial wave function used here. Their effect will be to enhance the tail of the momentum distribution with respect to the results provided by wave functions containing only scalar correlation factors. This can be verified for ^{40}Ca by comparing with the results of Ref. [27] where an extensive analysis of state-dependent correlations on both the nucleon density and momentum distribution was performed. In Ref. [6] the momentum distribution for *sp* nuclei was calculated by using the same nuclear potential and starting from both state dependent and state independent variational trial wave function and the effects of the former were analyzed.

Finally, the influence of the nuclear potential in the results can be estimated by comparing the results of this work for the one- and two-body densities and the momentum distribution with those of Refs. [13,28] for ^{40}Ca obtained from the FHNC at the single operator chain approximation by using the realistic Argonne v_8' and v_{14} two-nucleon potentials and the three-nucleon potentials of the Urbana class. The qualitative structure of the momentum distribution is the same with small quantitative differences as, for example, the position of the point where the change in slope occurs, which is shifted to lower k values when realistic potentials are used.

In Table IV, we show the excitation energy of some states of the ground state rotational band for the nuclei ^{20}Ne to ^{36}Ar calculated from the $\mathcal{JL}_o$ wave function. We also show the reduced transition probability between the 2^+ and the ground state. The results are compared with the experimental data [29], and with the noncorrelated values of the different quantities. With respect to the excitation energies, they compare better with the experimental ones if correlations among the nucleons are considered. In general the agreement with the experimental data can be considered as good, although in some cases the differences are appreciable. For example, the energy of the 2^+ state coincides, within the statistical error, for all the nuclei considered and does not follow the experimental trend. This is due to the limitations of the trial wave function used here and also to the fact that the nuclear force used is not realistic and therefore cannot provide accurate predictions. Nevertheless, the qualitative trend is reproduced. This is not the case for the reduced transition probability that is almost unchanged when correlations are taken into account. This quantity depends mainly on the model part of the wave function.

V. CONCLUSIONS

A variational study of the ground state and some members of its rotational band for spin-isospin saturated *sd* shell nuclei has been carried out. Trial wave functions including several aspects of the nuclear dynamics have been obtained and

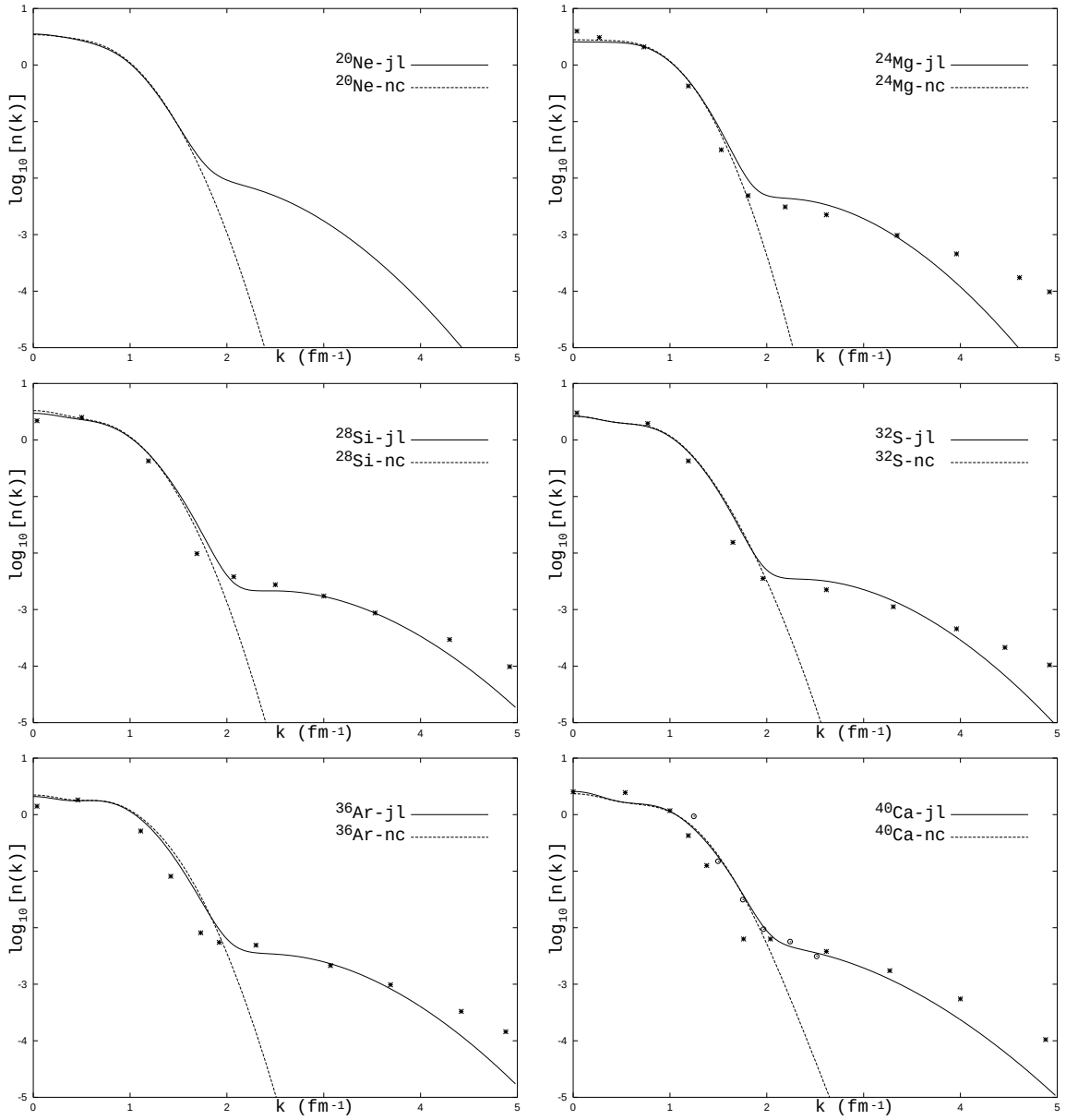

FIG. 6. Momentum distribution for all the nuclei studied calculated from both $\mathcal{JL}_o$ (jl) and noncorrelated (nc) wave functions. For ^{24}Mg, ^{28}Si, ^{32}S, ^{36}Ar, and ^{40}Ca, the two-body cluster expansion results of Ref. [25] (crosses) are shown. For ^{40}Ca the experimental results (circles) taken from Ref. [24] are also plotted. The units of k are fm^{-1}.

used to compute different properties. Short-range correlations are accounted by means of both a Jastrow and a linear correlation term. The model wave function includes deformation and provides the correct angular momentum quantum numbers of the nuclear state. Angular momentum projection has been carried out by rotating the intrinsic state and integrating over all angles weighted by the corresponding rotation matrix. The intrinsic states are built starting from the SU3 model.

One- and two-body radial densities have been calculated. A systematic analysis of the different correlation mechanisms included in our trial wave function has been carried out, focusing on the interplay between the Jastrow and the linear correlation terms. The results indicate that the effects induced by the latter not included in the former are small. The results for the one-body density show that this distribution function is governed by the model part of the trial function with a minor influence of the correlation factor. The two-body distribution presents stronger correlation effects, as it should be expected, with a structure that is similar for all of the cases considered here. A calculation for heavier nuclei using the optimal correlation factor obtained for ^{20}Ne gave accurate results. This is due to the fact that the correlation depends strongly on the nuclear interaction and the influence of the number of particles is less important for the nuclei studied here. The momentum distribution has been also calculated and the important effects of the nucleon-nucleon correlations for large-k values have been discussed. The results

TABLE IV. Excitation energies (in MeV) for some members of the ground state rotational band and reduced probability transition in fm^{-4} between the 2^+ and the ground state calculated from the $\mathcal{JL}_o$ trial wave function. The results are compared with the experimental ones (expt) of Ref. [29] and with the noncorrelated (nc) values.

	^{20}Ne	^{24}Mg	^{28}Si	^{32}S	^{36}Ar
$E(2^+)_{expt}$	1.63	1.37	1.78	2.23	1.97
$E(2^+)_o$	1.16 ± 0.11	1.14 ± 0.20	1.08 ± 0.20	1.35 ± 0.28	1.22 ± 0.36
$E(2^+)_{nc}$	0.66 ± 0.17	0.72 ± 0.25	0.69 ± 0.22	0.72 ± 0.30	1.06 ± 0.29
$E(4^+)_{expt}$	4.25	4.12	4.62	4.46	4.41
$E(4^+)_o$	4.34 ± 0.18	3.70 ± 0.24	3.61 ± 0.25	4.55 ± 0.32	4.82 ± 0.40
$E(4^+)_{nc}$	2.65 ± 0.23	2.69 ± 0.29	2.34 ± 0.24	2.52 ± 0.39	3.87 ± 0.45
$E(6^+)_{expt}$	8.78	8.11	8.54		9.68
$E(6^+)$	10.00 ± 0.38	7.76 ± 0.50	7.87 ± 0.32	9.74 ± 0.56	12.70 ± 0.97
$E(6^+)_{nc}$	6.82 ± 0.51	6.11 ± 0.56	5.21 ± 0.36	6.09 ± 0.74	10.1 ± 1.3
$E(8^+)_{expt}$	16.75	14.15			
$E(8^+)$	21.8 ± 1.4	13.62 ± 1.1	14.30 ± 0.64	11.5 ± 1.6	31.7 ± 4.5
$E(8^+)_{nc}$	14.7 ± 2.1	11.9 ± 1.5	10.32 ± 0.78	13.5 ± 1.9	27.0 ± 4.9
$B(2^+\rightarrow0^+;2)_{expt}$	96 ± 18	101 ± 17	63 ± 6	84 ± 8	
$B(2^+\rightarrow0^+;2)_o$	55.0 ± 0.4	94.6 ± 0.9	89.24 ± 0.8	87.2 ± 0.8	46.8 ± 0.5
$B(2^+\rightarrow0^+;2)_{nc}$	58.3 ± 0.4	99.8 ± 0.9	94.8 ± 0.7	88.8 ± 0.8	48.2 ± 0.5

show a good agreement with previous calculations and with the experimental results where available. Finally, the excitation energies of the ground state rotational band are better reproduced as correlations are taken into account, although the reduced transition probability between the 2^+ and the ground state is nearly independent of this part of the wave function. Also the experimental trend of the excitation energy of this state is not well described.

ACKNOWLEDGMENTS

This work was partially supported by the Ministerio de Ciencia y Tecnología and FEDER under Contract No. BFM2002-00200, and by the Junta de Andalucía. A.S. acknowledges the Italian MURST for financial support from Grant No. MIUR-2001025498. Some helpful discussions with F. Arias de Saavedra are acknowledged.

[1] A.N. Antonov, P.E. Hodgson, and I.Z. Petcov, *Nucleon Momentum and Density Distribution in Nuclei* (Clarendon, Oxford, 1988).
[2] R. Jastrow, Phys. Rev. **81**, 165 (1951).
[3] R. Jastrow, Phys. Rev. **98**, 1479 (1955).
[4] J.P. Elliot, Proc. R. Soc. London, Ser. A **245**, 128 (1958).
[5] R.F. Bishop, R. Guardiola, I. Moliner, J. Navarro, M. Portesi, A. Puente, and N.R. Walet, Nucl. Phys. **A643**, 243 (1998).
[6] E. Buendía, F.J. Gálvez, J. Praena, and A. Sarsa, J. Phys. G **26**, 1795 (2000).
[7] R.F. Bishop, M.N. Flynn, M.C. Boscá, E. Buendía, and R. Guardiola, Phys. Rev. C **42**, 1341 (1990).
[8] E. Buendía, F.J. Gálvez, J. Praena, and A. Sarsa, J. Phys. G **27**, 2211 (2001).
[9] R. Guardiola, I. Moliner, and M.A. Nagarajan, Nucl. Phys. **A679**, 393 (2001).
[10] E. Buendía, F.J. Gálvez, J. Praena, and A. Sarsa, Nucl. Phys. **A710**, 29 (2002).
[11] I. Moliner, N.R. Walet, and R.F. Bishop, J. Phys. G **28**, 1209 (2002).
[12] F. Arias de Saavedra, G. Co', A. Fabrocini, and S. Fantoni, Nucl. Phys. **A605**, 359 (1996).
[13] A. Fabrocini, F. Arias de Saavedra, and G. Co', Phys. Rev. C **61**, 044302 (2000).
[14] J.C. Owen, R.F. Bishop, and J.M. Irvine, Nucl. Phys. **A277**, 45 (1977).
[15] R.F. Bishop, C. Howes, J.M. Irvine, and M. Modarres, J. Phys. G **4**, 1709 (1978).
[16] E. Buendía and R. Guardiola, in *Condensed Matter Theories*, edited by L. Blum and F.B. Malik (Plenum, New York, 1993), Vol. 8, pp. 301–314.
[17] R.E. Peierls and J. Yoccoz, Proc. R. Soc. London, Ser. A **70**, 381 (1957).
[18] G. Ripka, in *Advances in Nuclear Physics*, edited by M. Baranger and E. Vogt (Plenum, New York, 1968), Vol. 1, pp. 183–259.
[19] W.H. Press, S.A. Teukolsky, W.T. Vettering, and B.P. Flannery, *Numerical Recipes in FORTRAN*: The Art of Scientific Computing (Cambridge University Press, Cambridge, 1992).
[20] I.R. Afnan and Y.C. Tang, Phys. Rev. **175**, 1337 (1968).
[21] R. Guardiola, in *Recent Progress in Many-Body Theories. Lecture Notes in Physics*, edited by J.G. Zabolitzky, M. de Llano, M. Fortes, and J.W. Clark (Springer-Verlag, Berlin, 1981), Vol. 142, pp. 398–406.
[22] R.B. Wiringa and S.C. Pieper, Phys. Rev. Lett. **89**, 182501 (2002).
[23] M.H. Kalos and P.A. Whitlock, *Monte Carlo Methods* (Wiley, New York, 1986).

[24] M.V. Stoitsov, A.N. Antonov, and S.S. Dimitrova, Phys. Rev. C **48**, 74 (1993).
[25] C.C. Moustakidis and S.E. Massen, Phys. Rev. C **62**, 034318 (2000).
[26] A. Sarsa, F.J. Gálvez, and E. Buendía, J. Phys. B: At. Mol. Opt. Phys. **32**, 2245 (1999).
[27] F. Arias de Saavedra, G. Co', and M.M. Renis, Phys. Rev. C **55**, 673 (1997).
[28] A. Fabrocini and G. Co', Phys. Rev. C **63**, 044319 (2001).
[29] R.B. Firestone, *Table of Isotopes*, 8th ed. (Wiley, New York, 1999).